ACS APPLIED MATERIALS & INTERFACES

www.acsami.org

Research Article

Wireless Single-Electrode Self-Powered Piezoelectric Sensor for Monitoring

Qi Liu,[#] Xiao-Xiong Wang,[#] Wei-Zhi Song, Hui-Jing Qiu, Jun Zhang, Zhiyong Fan, Miao Yu, and Yun-Ze Long*

Cite This: *ACS Appl. Mater. Interfaces* 2020, 12, 8288–8295

Read Online

ACCESS | Metrics & More | Article Recommendations | Supporting Information

ABSTRACT: In complex environments, there are often toxic and harmful conditions, and so self-powered sensors that use wireless access have a huge advantage. However, there is still a risk of short circuit for self-powered sensors in harsh environments. A single-electrode self-powered sensor was designed, which can be used to monitor body movements such as walking and running, as well as monitoring the motion of some mechanical devices, such as peristaltic pumps, door, and window switches. By using a threshold delay algorithm, this self-powered sensor can be connected to the phone to warn the phone user to check for theft or illegal intrusion when the door and window are opened. Further research shows that the single-electrode configuration can avoid the short-circuit behavior caused by device damage so that the self-powered sensor can still work even if it is pierced. Therefore, the wireless single-electrode self-powered sensor system has better reliability and is more applicable to harsh environments.

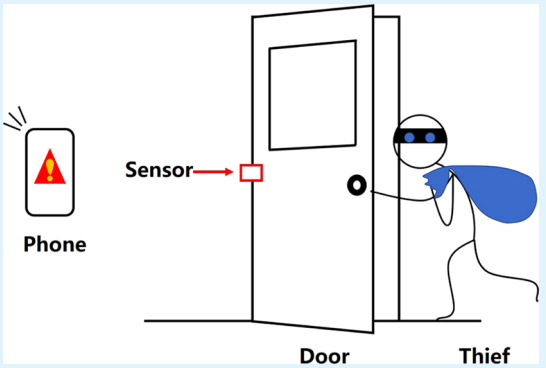

KEYWORDS: *nanogenerator, electrospinning, single electrode, sensor, wireless*

Downloaded via HONG KONG UNIV SCIENCE TECHLGY on August 23, 2020 at 17:35:19 (UTC).
See https://pubs.acs.org/sharingguidelines for options on how to legitimately share published articles.

1. INTRODUCTION

With the continuous advancement of related technologies of the Internet of Things, self-powered sensors have become widely popular.[1−5] Among them, nanogenerators have a wide range of potential applications.[6−19] They include piezoelectric,[20−25] pyroelectric,[26−30] and triboelectric sensors,[31−35] which convert environmental energy into electrical energy. Piezoelectric pressure sensors, pressure sensors based on piezoelectric nanogenerators (PENGs), have been extensively studied for their advantages of flexibility, low cost, and self-power supply.[36−41]

For nanogenerators, the structure of a single electrode broadens its range of applications, making it more suitable for people's daily lives.[42] Single-electrode nanogenerators offer greater flexibility, and the electrodeless side can touch anything such as skin,[43,44] pavement,[45] and raindrops[46] without affecting the device. However, most of the devices composed of single-electrode nanogenerators need to be grounded, which limits the flexibility of related devices to a certain extent.

Electrospinning is simple in a device, low in cost and capable of preparing nanofibers on a large scale. The reason is that the orientation of the electric dipole is induced by the electric field during the spinning process, and the high voltage and the volatilization, as well as the stretching of the solution, increase the β phase of poly(vinylidene fluoride) (PVDF), making electrospinning a convenient way of fabricating PENGs.

A single-electrode self-powered piezoelectric sensor based on electrospun PVDF PENG was fabricated. The single-electrode configuration reduces the possibility of short-circuit risk due to the electrode contact. A capacitor can be used to replace the ground wire, making it more portable. The reliability of the sensor in harsh environments was explored and the two-electrode sensor was used as a comparison. It has a wide range of potential applications. It can be used in wearable electronics to monitor body movements. After combining it with the wireless system, the phone's APP can monitor human motion in real time. It can be used to monitor the opening or closing of a door or window or a safe, which can improve the related safety. It can be used to monitor the working state of a peristaltic pump.

2. EXPERIMENTAL SECTION

2.1. Materials. Poly(vinylidene fluoride) (PVDF) powder ($M_w \sim$ 550 000) was provided by Shanghai 3F New Material Co., Ltd. (China). *N*,*N*-Dimethylformamide (DMF) was purchased from Sinopharm Chemical Reagents. Acetone was purchased from the

Received: November 25, 2019
Accepted: January 24, 2020
Published: January 24, 2020

© 2020 American Chemical Society

https://dx.doi.org/10.1021/acsami.9b21392
ACS Appl. Mater. Interfaces 2020, 12, 8288–8295

Laiyang Fine Chemical Factory, China. DMF and acetone are analytical reagents.

2.2. Electrospinning and Fabrication of Single-Electrode Self-Powered Piezoelectric Sensor. The PVDF powder was dissolved in a DMF/acetone solvent mixture (1:1 by weight) and then continuously stirred at 50 °C for 4 h to obtain a PVDF precursor solution (22 wt %).

The electrospinning of the solution was done using a syringe, and the advancement speed was adjusted to 16 μL/min by a syringe pump. A roller was used as a collector, and a voltage of 15 kV was applied between the needle and the roller at a distance of 15 cm. Electrospinning was carried out at room temperature at an ambient humidity of approximately 30%. A two-dimensional uniform electrospun PVDF nanofiber membrane (NFM) was obtained.

A suitable pressure was applied to the PVDF NFM to avoid the triboelectric effect, and an electrode was made on the PVDF NFM by ion sputtering to obtain a PVDF single-electrode self-powered piezoelectric sensor encapsulated with an aluminum foil and tape. It can also be unpackaged, which has no effect on device performance. The ground wire in the previous single-electrode structure is replaced with a capacitor so that the device can be free from the ground wire. The device is, therefore, portable.

2.3. Characterization. Characterization of the morphology and microstructure of PVDF NFM was carried out by scanning electron microscopy (SEM, JEOL, JSM-6700F). The diameter of the fiber was measured using the Nano Measurer software. The contact angle of the water was measured using a contact angle goniometer (Attension, Theta) to characterize its hydrophobicity. The stress−strain curve of the sample was tested by a universal testing machine (Instron-3300). The crystal structure of the sample was characterized by X-ray diffraction (XRD, Rigaku, Smartlab), Fourier transform infrared spectroscopy (FTIR, Thermo Scientific Nicolet iN10), and Raman spectroscopy (Labram HR 800, Jobin-Yvon Horiba, France). The change in the open-circuit voltage of the single-electrode self-powered piezoelectric sensor is collected by the digital multimeter (Rigol DM 3058). The response time of the sensor was measured by a digital oscilloscope (DSO-X 3024 A, Agilent). Homemade pressure equipment provides the periodic impact and bending to the sample. Wireless circuitry, including power converters, data conversion modules, signal acquisition, and amplification modules, is used to measure the wireless signals of the sensor. The wireless signal is finally received and demonstrated by a mobile phone.

3. RESULTS AND DISCUSSION

3.1. Basic Characteristics of Single-Electrode Self-Powered Piezoelectric Sensor. Figure 1a is a schematic view of electrospinning. Figure 1b shows a photograph of a single-electrode self-powered piezoelectric sensor based on an electrospun PVDF NFM. The SEM image of the PVDF NFM is shown in Figure 1c and the average fiber diameter is 1.01 μm. The measurement of the water contact angle of the sample is shown in Figure 1d. The water contact angle is about 144.03°, showing good hydrophobic properties and certain self-cleaning performance. Figure 1e shows the stress−strain curve of the sample after tensile testing. The elongation of the sample is about 77.15% and the tensile strength is about 10.24 MPa, which has a certain antidamage effect.

The XRD pattern (Figure 2a), FTIR spectrum (Figure 2b), and Raman spectrum (Figure 2c) reveal the crystal phase of the PVDF NFM. The XRD pattern (Figure 2a) and the FTIR spectrum (Figure 2b) of the PVDF powder before electrospinning were tested for comparison. The PVDF powder before electrospinning exhibits a peak of θ = 18.8°, corresponding to the (020) reflection, and a peak of θ = 20.2°, corresponding to the (110) reflection of the nonpolar α phase.[47] The two peaks of the PVDF NFM show a significant drop, with the appearance of a new peak of 2θ = 20.4°,

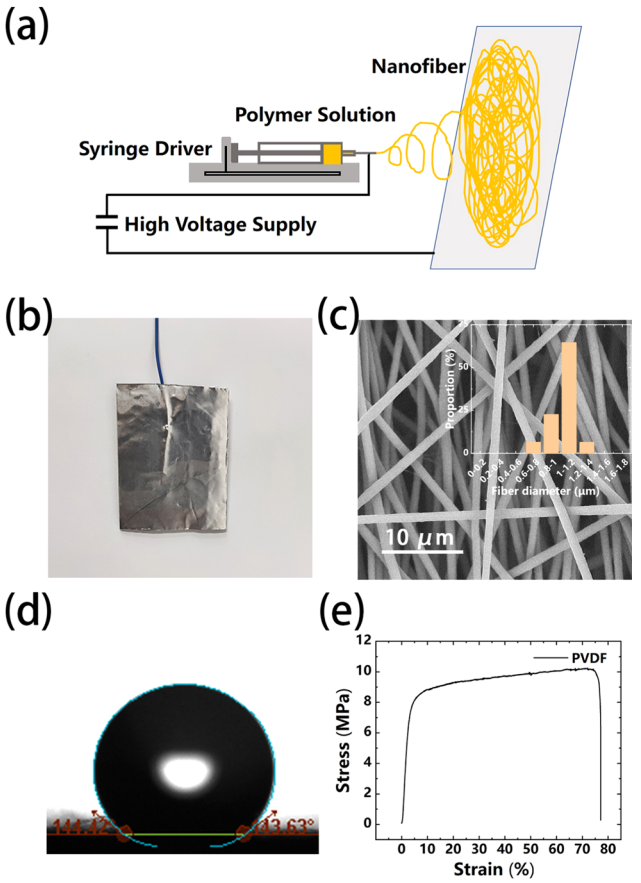

Figure 1. (a) Schematic view of electrospinning. (b) Photograph of the packaged single-electrode self-powered piezoelectric sensor. (c) SEM image and fiber size distribution bar graph of the PVDF NFM. (d) Water contact angle of the PVDF NFM. (e) Stress−strain curve of the PVDF NFM.

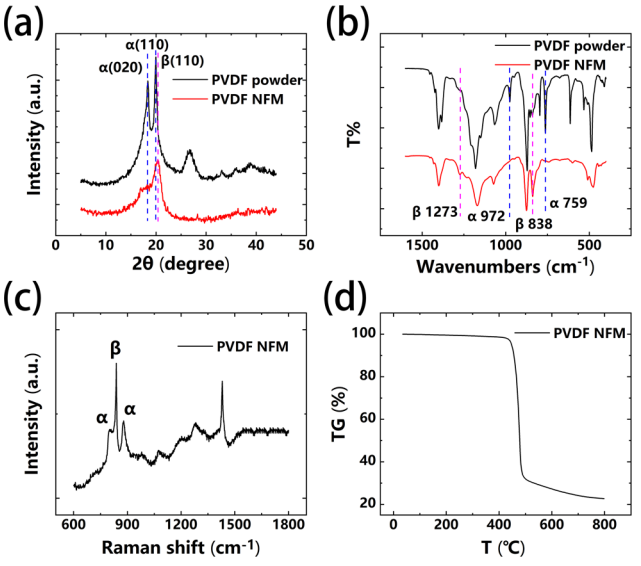

Figure 2. (a) XRD pattern of the PVDF NFM and PVDF powders. (b) FTIR spectrum of the PVDF NFM and PVDF powders. (c) Raman spectrum of the PVDF NFM. (d) TG pattern of the PVDF NFM.

corresponding to the (110) reflection of the electroactive β phase.[48,49] Similarly, in the FTIR spectrum of Figure 2b, the

https://dx.doi.org/10.1021/acsami.9b21392
ACS Appl. Mater. Interfaces 2020, 12, 8288−8295

PVDF powder exhibited characteristic peaks at 759 and 972 cm^{-1}, corresponding to the α phase. The two peaks of the PVDF NFM decreased significantly, while the peaks appear at 838 and 1272 cm^{-1}, corresponding to the generation of the β phase.[50] Also, in the PVDF NFM Raman spectrum, the significant presence of the β phase was again verified. These show that electrospinning promotes the conversion of PVDF from the α phase to the β phase.[51,52] The reason is that during the electrospinning process, the high-voltage electric field polarizes and stretches the PVDF fibers, and the rapid evaporation of the solvent facilitates the formation of PVDF β phase.[53−55] The TG pattern of PVDF NFM (Figure 2d) shows that the thermal decomposition temperature of PVDF NFM at 5% weight loss is 447 °C.

3.2. Piezoelectricity of Single-Electrode Self-Powered Piezoelectric Sensor. The piezoelectric principle of the single-electrode self-powered piezoelectric sensor is shown in Figure 3. In the single-electrode structure,[44] we replaced the ground wire with a large capacitor. This device gets rids of the ground wire and is more portable. Only one connection line is needed, which can be conveniently placed in the device and circuit, occupying only a small space. It can reduce the possibility of short-circuit damage to the device due to the contact between the lines. It can work normally even after the electrode is broken; of course, the security of the device is also improved.

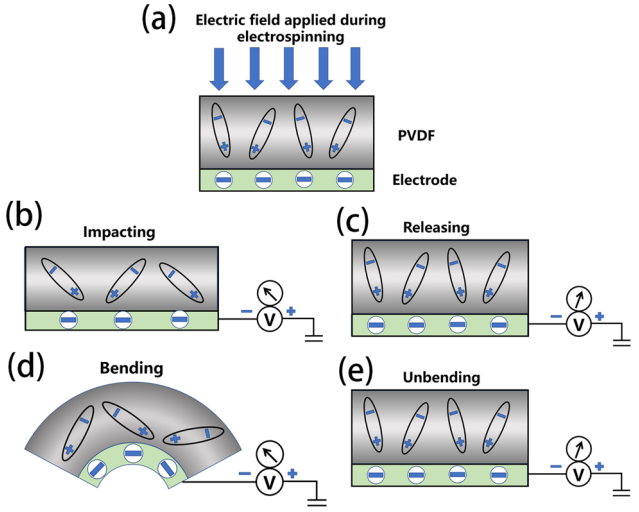

Figure 3. (a) Orientation of the electric dipole and the schematic diagram of the structure of PVDF NFM. (b, c) Piezoelectric output that applies impact and releases strain. (d, e) Piezoelectric output that applies bending and strain relief.

As shown in Figure 3a, the electrospinning process spontaneously polarizes PVDF, and the PVDF electroactive dipole is induced to be oriented in the direction of the electric field, that is, in the thickness direction of the membrane.[56,57] The electric dipole is in equilibrium and its total spontaneous polarization has a constant average intensity.[58,59] When the sensor is impacted, PVDF NFM is compressed and the total spontaneous polarization is greatly reduced, creating an open-circuit voltage (Figure 3b). Conversely, the total spontaneous polarization of the PVDF NFM is restored when the impact is released and an opposite voltage signal appears, as shown in Figure 3c. Piezoelectric open-circuit voltage can be expressed by the equation

$$V_{\text{piezo}} = A \times \frac{d_{33}}{\varepsilon_{33}^{T}} \times h \times \Delta\sigma \quad (1)$$

where A, d_{33}, ε_{33}^{T}, h, and $\Delta\sigma$ are the effective area of the device, the piezoelectric coefficient, permittivity, thickness, and mechanical stress, respectively.[60] The bending of the PVDF NFM results in a decrease in the polarization in the direction of polarization,[6] resulting in an open-circuit voltage (Figure 3d). The opposite signal is produced upon release (Figure 3e).

The sensor piezoelectric signal is tested by a self-made pressure device.[35] The sensor has no output signal when there is no disturbance. Figure 4a−c is the voltage output signal of the sensor at different pressures. The applied pressure is about 3, 9, and 12 N, respectively, and the frequency is about 0.07 Hz. The sensor outputs a stable square-wave signal and the output voltage increases with pressure. Figure 4d−g shows the output signal of the sensor under repeated bending at different frequencies. The frequencies are 0.75, 1.5, 2.25, and 3 Hz, respectively. The bending angle is about 70°. The sensor outputs a stable pulse signal and the output voltage increases with frequency. These data also show that the single-electrode self-powered piezoelectric sensor has good durability and stability. The sensor's sensitivity is demonstrated by the output of the sensor under the pressure of different weights (Figure S1, Supporting Information). The response time of the sensor was measured by a digital oscilloscope (Figure S2, Supporting Information).

3.3. Monitoring Human Motion Data in Conjunction with Wireless Systems. Piezoelectric devices can monitor certain movements of the human body. We combine the wireless system with the single-electrode self-powered piezoelectric sensor, which can receive the piezoelectric signal of the sensor with a mobile phone and monitor the motion data of the human body in real time. The wireless system comprises a signal acquisition and amplification module, a power converter, a data conversion control module, and a Bluetooth module, which, respectively, correspond to 1, 2, 3, and 4 in Figure 5a. The wireless system can collect and amplify the piezoelectric signal and then convert the signal into a digital signal and transmit it to the mobile phone via Bluetooth.[61] The final signal is displayed by an APP (only a positive value is designed and the refresh rate is relatively low). The wireless system measures approximately 40 mm × 50 mm × 2 mm. The sensor is placed in the heel position of the insole and the wireless system is taped to the inside of the garment. The two are connected by wires. The piezoelectric signals for walking and running are then collected and are shown in Figure 5b,c, respectively (see Videos S1 and S2, Supporting Information). It is worth noting that each step in the walk produces three signals (Figure 5b). The first signal 1 is generated when the foot falls on the ground, and the last two signals 2 and 3 are generated when the foot is lifted. There are two processes in the action of lifting the foot. When the heel leaves the ground, while the toe still touches the ground, one signal is generated. Then, the toe also leaves the ground and the shoe will collide with the heel, resulting in another one. A slight swing of the foot will also produce some small peaks. This sensor can be conveniently placed in any shoe or clothing without compromising comfort. Of course, this combined with a wireless system provides a means of connecting this sensor to the Internet of Things.

3.4. Monitor the Opening or Closing of Doors, Windows, Safes, etc. Safety has always been a matter of

https://dx.doi.org/10.1021/acsami.9b21392
ACS Appl. Mater. Interfaces 2020, 12, 8288−8295

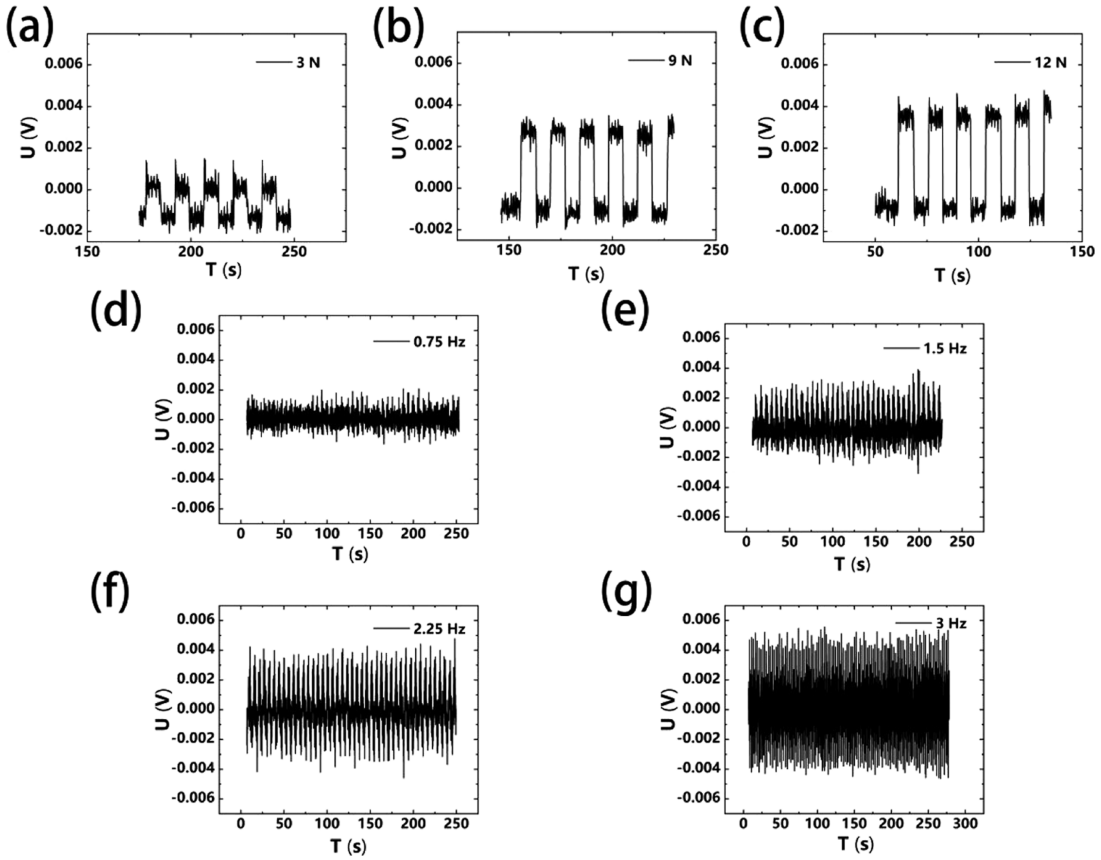

Figure 4. Open-circuit voltage signal of the single-electrode self-powered piezoelectric sensor. (a–c) Output by applying different pressures at a frequency of 0.07 Hz. (d–g) Output by repeated bending at different frequencies.

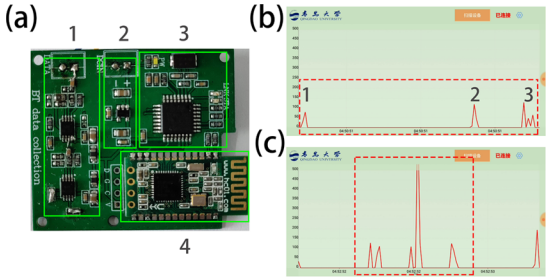

Figure 5. (a) Photograph of the wireless system. 1, 2, 3, and 4 are signal acquisition and amplification module, power converter, data conversion control module, and Bluetooth module, respectively. (b) Signals for walking; within the red dotted box is the signal of a step. (c) Signals for running; within the red dotted box is the signal of a step.

great concern. The single-electrode self-powered piezoelectric sensor can monitor some safety-related things and prevent theft of items. It monitors the opening and closing of doors or windows. An alarm is issued when the door or window is accidentally opened. The sensor is attached to the hinged side of the door and window (Figure 6a), either inside or outside. When the door or window is opened or closed, the sensor is bent and outputs a piezoelectric signal. We collected the piezoelectric signals for fast (about 1 s) and slow (about 3 s) opening or closing the door, as shown in Figure 6b. We have written a threshold algorithm. The threshold and time can be set reasonably. The threshold system can illuminate a red light to alert when a door or window is opened (see Video S3, Supporting Information). Other alarm systems can be connected as an alarm signal. Similarly, our sensors can also monitor other hinged things such as safes. It can also be used to monitor the opening or closing of push-pull windows. The sensor is attached to one side of the window, as shown in Figure 6c. When the window is opened or closed, the sensor will be given a momentary force and an output signal (Figure 6d). Of course, the sensor can be connected to the Bluetooth device, and a mobile phone can be used to monitor the opening or closing of a door or window or a safe in real time. The sensors can also be connected to the Internet of Things that has always been the focus of attention.

Because of the large force at the hinge, the sensor attached here is easily broken partially. Then, the signal output of the single-electrode self-powered piezoelectric sensor under the broken state of the electrode was studied and compared with the two-electrode sensor. The signal is acquired under the same conditions (same amplitude and frequency as of opening the door). Figure 6e is an output signal of the single-electrode sensor monitoring the opening or closing of a door in a normal state. Figure 6f is the output signal of the single-electrode sensor after the electrode is broken. There is no significant change in the output signal. In the two-electrode sensor, after the two electrodes are partially cracked, it is inevitable that the two electrodes touch each other and cause short-circuit. Figure 6g is an output signal of the two-electrode sensor monitoring the door opening or closing in a normal state. Figure 6h is the output signal of the two-electrode sensor after the electrode is broken and shorted. Because the two electrodes are shorted to each other, the output signal of the two-electrode sensor

https://dx.doi.org/10.1021/acsami.9b21392
ACS Appl. Mater. Interfaces 2020, 12, 8288–8295

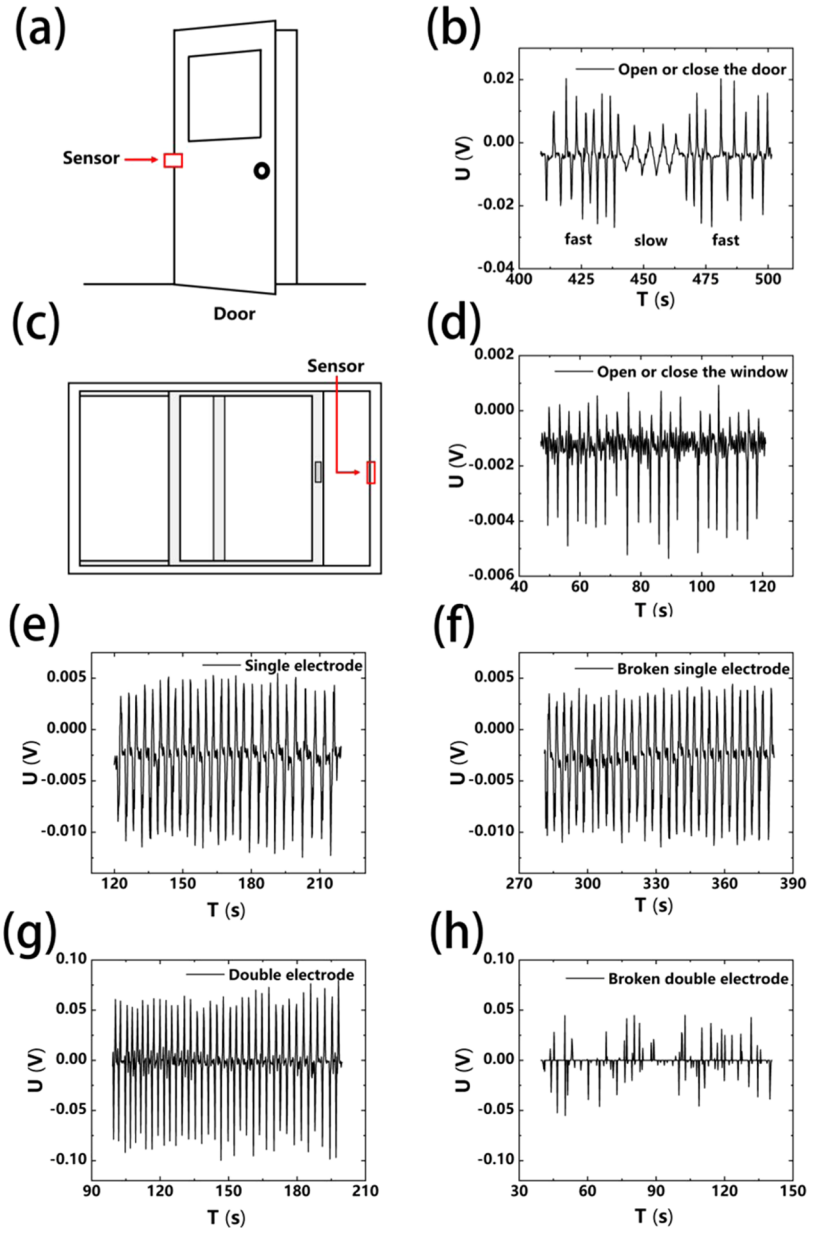

Figure 6. (a) Sensor attached to the hinged side of the door. (b) Piezoelectric signals for fast (about 1 s) and slow (about 3 s) opening or closing of the door. (c) Sensor attached to one side of the window. (d) Piezoelectric signal of the opening or closing of push-pull windows. (e, f) Output signal of the single-electrode piezoelectric sensor before and after electrode breakage. (g, h) Output signal of the two-electrode piezoelectric sensor before and after electrode breakage.

produces a partial loss that becomes cluttered. In other words, this single-electrode piezoelectric sensor can be more reliable than a two-electrode sensor in harsh environments.

3.5. Monitor the Working State of the Peristaltic Pump. To demonstrate the wide range of potential applications for sensors, it has been tested for use on other instruments. The peristaltic pump can finely control the flow of liquid and is often used in chemical, pharmaceutical, medical, and other fields. Blockage often occurs due to its working principle and working environment. If it cannot be found on time, it will have a big impact on people's work. Our single-electrode self-powered piezoelectric sensor provides such help. This sensor can monitor the working state of the peristaltic pump. The sensor can be placed between the inner wall of the pump head and the pump tube, and a piezoelectric signal is generated each time the roller squeezes the pump tube to push the liquid. We use a weight to roll a section of the water pipe to simulate the process of the roller squeezing the pump tube. The water pipe is placed on the sensor to simulate the working state of the sensor in the peristaltic pump. Figure 7 is a piezoelectric signal of the simulation of the peristaltic pump operation. We have written a threshold algorithm. When the peristaltic pump stops working unexpectedly, the program will light the indicator light to give an alarm signal (see Video S4, Supporting Information). Because the sensor is light and flexible, it does not affect the operation of the peristaltic pump and can alert when the peristaltic pump stops working. Due to its portability and single electrode, it can be moved anywhere as needed without damage. It can also be monitored in real time by mobile phone via a Bluetooth device.

https://dx.doi.org/10.1021/acsami.9b21392
ACS Appl. Mater. Interfaces 2020, 12, 8288−8295

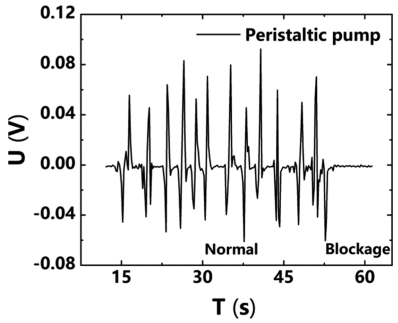

Figure 7. Piezoelectric signal of simulation about peristaltic pump operation.

4. CONCLUSIONS

A single-electrode self-powered piezoelectric sensor based on electrospun PVDF PENG was fabricated. Single-electrode sensors have been found to exhibit higher reliability than two-electrode sensors in harsh environments. Unlike a two-electrode piezoelectric sensor, it can work normally even after the electrode is broken. It can monitor human motion data, monitor the opening and closing of doors or windows or safes, and monitor the working state of the peristaltic pump. The threshold system is used to issue alerts in a timely manner, and the wireless system is used to transmit real-time data to the handset. Moreover, the sensor is light, soft, and portable and is not easily damaged or malfunctioned and can be manufactured at a low cost and on a large scale.

■ ASSOCIATED CONTENT

Supporting Information

The Supporting Information is available free of charge at https://pubs.acs.org/doi/10.1021/acsami.9b21392.

Voltage output with different weights applied to the same area on the sensor; the response time of the sensor (Figures S1 and S2) (PDF)

The signals for walking (sensor in right shoe) (Video S1) (MP4)

The signals for running (sensor in right shoe) (Video S2) (MP4)

Illumination of red light to alert when a door is opened (Video S3) (MP4)

Illumination of red light to alert when the peristaltic pump stops working (Video S4) (MP4)

■ AUTHOR INFORMATION

Corresponding Author

Yun-Ze Long − *Collaborative Innovation Center for Nanomaterials & Devices, College of Physics, Qingdao University, Qingdao 266071, China;* orcid.org/0000-0002-4278-4515; Phone: +86 139 5329 0681; Email: yunze.long@163.com

Authors

Qi Liu − *Collaborative Innovation Center for Nanomaterials & Devices, College of Physics, Qingdao University, Qingdao 266071, China*

Xiao-Xiong Wang − *Collaborative Innovation Center for Nanomaterials & Devices, College of Physics, Qingdao University, Qingdao 266071, China*

Wei-Zhi Song − *Collaborative Innovation Center for Nanomaterials & Devices, College of Physics, Qingdao University, Qingdao 266071, China*

Hui-Jing Qiu − *Collaborative Innovation Center for Nanomaterials & Devices, College of Physics, Qingdao University, Qingdao 266071, China*

Jun Zhang − *Collaborative Innovation Center for Nanomaterials & Devices, College of Physics, Qingdao University, Qingdao 266071, China*

Zhiyong Fan − *Department of Electronic & Computer Engineering, The Hong Kong University of Science & Technology, Kowloon 999077, Hong Kong, China;* orcid.org/0000-0002-5397-0129

Miao Yu − *Collaborative Innovation Center for Nanomaterials & Devices, College of Physics, Qingdao University, Qingdao 266071, China; Department of Mechanical Engineering, Columbia University, New York, New York 10027, United States*

Complete contact information is available at: https://pubs.acs.org/10.1021/acsami.9b21392

Author Contributions

#These authors contributed equally to this work.

Notes

The authors declare no competing financial interest.

■ ACKNOWLEDGMENTS

This work was supported by the National Natural Science Foundation of China (51673103 and 11847135), the Shandong Provincial Natural Science Foundation, China (ZR2017BA013), and the China Postdoctoral Science Foundation (2017M612200).

■ REFERENCES

(1) Wang, Z. L. On Maxwell's Displacement Current for Energy and Sensors: the Origin of Nanogenerators. *Mater. Today* **2017**, *20*, 74−82.

(2) Jin, L.; Chen, J.; Zhang, B.; Deng, W.; Zhang, L.; Zhang, H.; Huang, X.; Zhu, M.; Yang, W.; Wang, Z. L. Self-Powered Safety Helmet Based on Hybridized Nanogenerator for Emergency. *ACS Nano* **2016**, *10*, 7874−7881.

(3) Zhang, B.; Chen, J.; Jin, L.; Deng, W.; Zhang, L.; Zhang, H.; Zhu, M.; Yang, W.; Wang, Z. L. Rotating-Disk-Based Hybridized Electromagnetic−Triboelectric Nanogenerator for Sustainably Powering Wireless Traffic Volume Sensors. *ACS Nano* **2016**, *10*, 6241−6247.

(4) Zhang, N.; Tao, C.; Fan, X.; Chen, J. Progress in Triboelectric Nanogenerators as Self-Powered Smart Sensors. *J. Mater. Res.* **2017**, *32*, 1628−1646.

(5) Lin, Z.; Chen, J.; Li, X.; Zhou, Z.; Meng, K.; Wei, W.; Yang, J.; Wang, Z. L. Triboelectric Nanogenerator Enabled Body Sensor Network for Self-Powered Human Heart-Rate Monitoring. *ACS Nano* **2017**, *11*, 8830−8837.

(6) Ko, Y. J.; Kim, D. Y.; Won, S. S.; Ahn, C. W.; Kim, I. W.; Kingon, A. I.; Kim, S.-H.; Ko, J.-H.; Jung, J. H. Flexible $Pb(Zr_{0.52}Ti_{0.48})O_3$ Films for a Hybrid Piezoelectric-Pyroelectric Nanogenerator under Harsh Environments. *ACS Appl. Mater. Interfaces* **2016**, *8*, 6504−6511.

(7) Guo, H.; He, X.; Zhong, J.; Zhong, Q.; Leng, Q.; Hu, C.; Chen, J.; Tian, L.; Xi, Y.; Zhou, J. A Nanogenerator for Harvesting Airflow Energy and Light Energy. *J. Mater. Chem. A* **2014**, *2*, 2079−2087.

(8) Zhang, L.; Zhang, B.; Chen, J.; Jin, L.; Deng, W.; Tang, J.; Zhang, H.; Pan, H.; Zhu, M.; Yang, W.; Wang, Z. L. Lawn Structured Triboelectric Nanogenerators for Scavenging Sweeping Wind Energy on Rooftops. *Adv. Mater.* **2016**, *28*, 1650−1656.

(9) Zheng, L.; Cheng, G.; Chen, J.; Lin, L.; Wang, J.; Liu, Y.; Li, H.; Wang, Z. L. A Hybridized Power Panel to Simultaneously Generate Electricity from Sunlight, Raindrops, and Wind around the Clock. *Adv. Energy Mater.* **2015**, *5*, No. 1501152.
(10) Yang, Y.; Zhu, G.; Zhang, H.; Chen, J.; Zhong, X.; Lin, Z.-H.; Su, Y.; Bai, P.; Wen, X.; Wang, Z. L. Triboelectric Nanogenerator for Harvesting Wind Energy and as Self-Powered Wind Vector Sensor System. *ACS Nano* **2013**, *7*, 9461−9468.
(11) Seung, W.; Gupta, M. K.; Lee, K. Y.; Shin, K.-S.; Lee, J.-H.; Kim, T. Y.; Kim, S.; Lin, J.; Kim, J. H.; Kim, S.-W. Nanopatterned Textile-Based Wearable Triboelectric Nanogenerator. *ACS Nano* **2015**, *9*, 3501−3509.
(12) Kim, K. N.; Chun, J.; Kim, J. W.; Lee, K. Y.; Park, J.-U.; Kim, S.-W.; Wang, Z. L.; Baik, J. M. Highly Stretchable 2D Fabrics for Wearable Triboelectric Nanogenerator under Harsh Environments. *ACS Nano* **2015**, *9*, 6394−6400.
(13) Li, Z.; Shen, J.; Abdalla, I.; Yu, J.; Ding, B. Nanofibrous Membrane Constructed Wearable Triboelectric Nanogenerator for High Performance Biomechanical Energy Harvesting. *Nano Energy* **2017**, *36*, 341−348.
(14) Wu, W.; Bai, S.; Yuan, M.; Qin, Y.; Wang, Z. L.; Jing, T. Lead Zirconate Titanate Nanowire Textile Nanogenerator for Wearable Energy-Harvesting and Self-Powered Devices. *ACS Nano* **2012**, *6*, 6231−6235.
(15) Bai, P.; Zhu, G.; Jing, Q.; Yang, J.; Chen, J.; Su, Y.; Ma, J.; Zhang, G.; Wang, Z. L. Membrane-based Self-Powered Triboelectric Sensors for Pressure Change Detection and its Uses in Security Surveillance and Healthcare Monitoring. *Adv. Funct. Mater.* **2014**, *24*, 5807−5813.
(16) Yang, J.; Chen, J.; Su, Y.; Jing, Q.; Li, Z.; Yi, F.; Wen, X.; Wang, Z.; Wang, Z. L. Eardrum-Inspired Active Sensors for Self-Powered Cardiovascular System Characterization and Throat-Attached Anti-Interference Voice Recognition. *Adv. Mater.* **2015**, *27*, 1316−1326.
(17) Yang, W.; Chen, J.; Wen, X.; Jing, Q.; Yang, J.; Su, Y.; Zhu, G.; Wu, W.; Wang, Z. L. Triboelectrification Based Motion Sensor for Human-Machine Interfacing. *ACS Appl. Mater. Interfaces* **2014**, *6*, 7479−7484.
(18) Yi, F.; Lin, L.; Niu, S.; Yang, P. K.; Wang, Z.; Chen, J.; Zhou, Y.; Zi, Y.; Wang, J.; Liao, Q.; et al. Stretchable-Rubber-Based Triboelectric Nanogenerator and its Application as Self-Powered Body Motion Sensors. *Adv. Funct. Mater.* **2015**, *25*, 3688−3696.
(19) Song, W.-Z.; Wang, X.-X.; Qiu, H.-J.; Liu, Q.; Zhang, J.; Fan, Z.; Yu, M.; Ramakrishna, S.; Hu, H.; Long, Y.-Z. Sliding Non-Contact Inductive Nanogenerator. *Nano Energy* **2019**, *63*, No. 103878.
(20) Serairi, L.; Gu, L.; Qin, Y.; Lu, Y.; Basset, P.; Leprince-Wang, Y. Flexible Piezoelectric Nanogenerators Based on PVDF-TrFE Nanofibers. *Eur. Phys. J. Appl. Phys.* **2017**, *80*, No. 30901.
(21) Karan, S. K.; Bera, R.; Paria, S.; Das, A. K.; Maiti, S.; Maitra, A.; Khatua, B. B. An Approach to Design Highly Durable Piezoelectric Nanogenerator Based on Self-Poled PVDF/AlO-rGO Flexible Nanocomposite with High Power Density and Energy Conversion Efficiency. *Adv. Energy Mater.* **2016**, *6*, No. 1601016.
(22) Siddiqui, S.; Lee, H. B.; Kim, D. I.; Duy, L. T.; Hanif, A.; Lee, N. E. An Omnidirectionally Stretchable Piezoelectric Nanogenerator Based on Hybrid Nanofibers and Carbon Electrodes for Multimodal Straining and Human Kinematics Energy Harvesting. *Adv. Energy Mater.* **2018**, *8*, No. 1701520.
(23) Wu, W. High-Performance Piezoelectric Nanogenerators for Self-Powered Nanosystems: Quantitative Standards and Figures of Merit. *Nanotechnology* **2016**, *27*, No. 112503.
(24) Baek, S.-H.; Park, I.-K. Flexible Piezoelectric Nanogenerators Based on a Transferred ZnO Nanorod/Si Micro-Pillar Array. *Nanotechnology* **2017**, *28*, No. 095401.
(25) Wang, X.; Song, W.-Z.; You, M.-H.; Zhang, J.; Yu, M.; Fan, Z.; Ramakrishna, S.; Long, Y.-Z. Bionic Single-Electrode Electronic Skin Unit Based on Piezoelectric Nanogenerator. *ACS Nano* **2018**, *12*, 8588−8596.
(26) Yang, Y.; Zhou, Y.; Wu, J. M.; Wang, Z. L. Single Micro/Nanowire Pyroelectric Nanogenerators as Self-Powered Temperature Sensors. *ACS Nano* **2012**, *6*, 8456−8461.
(27) Wang, X.; Dai, Y.; Liu, R.; He, X.; Li, S.; Wang, Z. L. Light-Triggered Pyroelectric Nanogenerator Based on a Pn-Junction for Self-powered Near-Infrared Photosensing. *ACS Nano* **2017**, *11*, 8339−8345.
(28) Gao, F.; Li, W.; Wang, X.; Fang, X.; Ma, M. A Self-Sustaining Pyroelectric Nanogenerator Driven by Water Vapor. *Nano Energy* **2016**, *22*, 19−26.
(29) Qi, J.; Ma, N.; Yang, Y. Photovoltaic−Pyroelectric Coupled Effect Based Nanogenerators for Self-Powered Photodetector System. *Adv. Mater. Interfaces* **2018**, *5*, No. 1701189.
(30) You, M.-H.; Wang, X.-X.; Yan, X.; Zhang, J.; Song, W.-Z.; Yu, M.; Fan, Z.-Y.; Ramakrishna, S.; Long, Y.-Z. A Self-Powered Flexible Hybrid Piezoelectric−Pyroelectric Nanogenerator Based on Non-Woven Nanofiber Membranes. *J. Mater. Chem. A* **2018**, *6*, 3500−3509.
(31) Quan, Z.; Han, C. B.; Jiang, T.; Wang, Z. L. Robust Thin Films-Based Triboelectric Nanogenerator Arrays for Harvesting Bidirectional Wind Energy. *Adv. Energy Mater.* **2016**, *6*, No. 1501799.
(32) Dai, K.; Wang, X.; Yi, F.; Jiang, C.; Li, R.; You, Z. Triboelectric Nanogenerators as Self-Powered Acceleration Sensor under High-g Impact. *Nano Energy* **2018**, *45*, 84−93.
(33) Pan, R.; Xuan, W.; Chen, J.; Dong, S.; Jin, H.; Wang, X.; Li, H.; Luo, J. Fully Biodegradable Triboelectric Nanogenerators Based on Electrospun Polylactic Acid and Nanostructured Gelatin Films. *Nano Energy* **2018**, *45*, 193−202.
(34) Xu, W.; Huang, L. B.; Wong, M. C.; Chen, L.; Bai, G.; Hao, J. Environmentally Friendly Hydrogel-Based Triboelectric Nanogenerators for Versatile Energy Harvesting and Self-Powered Sensors. *Adv. Energy Mater.* **2017**, *7*, No. 1601529.
(35) Qiu, H.-J.; Song, W.-Z.; Wang, X.-X.; Zhang, J.; Fan, Z.; Yu, M.; Ramakrishna, S.; Long, Y.-Z. A Calibration-Free Self-Powered Sensor for Vital Sign Monitoring and Finger Tap Communication Based on Wearable Triboelectric Nanogenerator. *Nano Energy* **2019**, *58*, 536−542.
(36) Chun, J.; Lee, K. Y.; Kang, C. Y.; Kim, M. W.; Kim, S. W.; Baik, J. M. Embossed Hollow Hemisphere-Based Piezoelectric Nanogenerator and Highly Responsive Pressure Sensor. *Adv. Funct. Mater.* **2014**, *24*, 2038−2043.
(37) Zhang, Y.; Yang, Y.; Gu, Y.; Yan, X.; Liao, Q.; Li, P.; Zhang, Z.; Wang, Z. Performance and Service Behavior in 1-D Nanostructured Energy Conversion Devices. *Nano Energy* **2015**, *14*, 30−48.
(38) Bowen, C.; Kim, H.; Weaver, P.; Dunn, S. Piezoelectric and Ferroelectric Materials and Structures for Energy Harvesting Applications. *Energy Environ. Sci.* **2014**, *7*, 25−44.
(39) Wu, W.; Wang, Z. L. Piezotronics and Piezo-Phototronics for Adaptive Electronics and Optoelectronics. *Nat. Rev. Mater.* **2016**, *1*, No. 16031.
(40) Liu, S.; Wang, L.; Wang, Z.; Cai, Y.; Feng, X.; Qin, Y.; Wang, Z. L. Double-Channel Piezotronic Transistors for Highly Sensitive Pressure Sensing. *ACS Nano* **2018**, *12*, 1732−1738.
(41) Shi, K.; Sun, B.; Huang, X.; Jiang, P. Synergistic Effect of Graphene Nanosheet and $BaTiO_3$ Nanoparticles on Performance Enhancement of Electrospun PVDF Nanofiber Mat for Flexible Piezoelectric Nanogenerators. *Nano Energy* **2018**, *52*, 153−162.
(42) Chen, J.; Ding, P.; Pan, R.; Xuan, W.; Guo, D.; Ye, Z.; Yin, W.; Jin, H.; Wang, X.; Dong, S.; Luo, J. Self-Powered Transparent Glass-Based Single Electrode Triboelectric Motion Tracking Sensor Array. *Nano Energy* **2017**, *34*, 442−448.
(43) Yang, Y.; Zhang, H.; Lin, Z.-H.; Zhou, Y. S.; Jing, Q.; Su, Y.; Yang, J.; Chen, J.; Hu, C.; Wang, Z. L. Human Skin Based Triboelectric Nanogenerators for Harvesting Biomechanical Energy and as Self-Powered Active Tactile Sensor System. *ACS Nano* **2013**, *7*, 9213−9222.
(44) Yang, Y.; Zhou, Y. S.; Zhang, H.; Liu, Y.; Lee, S.; Wang, Z. L. A Single-Electrode Based Triboelectric Nanogenerator as Self-Powered Tracking System. *Adv. Mater.* **2013**, *25*, 6594−6601.

https://dx.doi.org/10.1021/acsami.9b21392
ACS Appl. Mater. Interfaces 2020, 12, 8288−8295

(45) Mao, Y.; Geng, D.; Liang, E.; Wang, X. Single-Electrode Triboelectric Nanogenerator for Scavenging Friction Energy from Rolling Tires. *Nano Energy* **2015**, *15*, 227−234.
(46) Liang, Q.; Yan, X.; Liao, X.; Zhang, Y. Integrated Multi-Unit Transparent Triboelectric Nanogenerator Harvesting Rain Power for Driving Electronics. *Nano Energy* **2016**, *25*, 18−25.
(47) Park, Y. J.; Kang, Y. S.; Park, C. Micropatterning of Semicrystalline Poly (Vinylidene Fluoride)(PVDF) Solutions. *Eur. Polym. J.* **2005**, *41*, 1002−1012.
(48) Fang, J.; Niu, H.; Wang, H.; Wang, X.; Lin, T. Enhanced Mechanical Energy Harvesting Using Needleless Electrospun Poly (Vinylidene Fluoride) Nanofibre Webs. *Energy Environ. Sci.* **2013**, *6*, 2196−2202.
(49) Wang, S.; Wang, Z. L.; Yang, Y. A One-Structure-Based Hybridized Nanogenerator for Scavenging Mechanical and Thermal Energies by Triboelectric−Piezoelectric−Pyroelectric Effects. *Adv. Mater.* **2016**, *28*, 2881−2887.
(50) Martins, P.; Lopes, A.; Lanceros-Mendez, S. Electroactive Phases of Poly (Vinylidene Fluoride): Determination, Processing and Applications. *Prog. Polym. Sci.* **2014**, *39*, 683−706.
(51) Fang, J.; Wang, X.; Lin, T. Electrical Power Generator from Randomly Oriented Electrospun Poly (Vinylidene Fluoride) Nanofibre Membranes. *J. Mater. Chem.* **2011**, *21*, 11088−11091.
(52) Gheibi, A.; Latifi, M.; Merati, A. A.; Bagherzadeh, R. Piezoelectric Electrospun Nanofibrous Materials for Self-Powering Wearable Electronic Textiles Applications. *J. Polym. Res.* **2014**, *21*, No. 469.
(53) Dhakras, D.; Borkar, V.; Ogale, S.; Jog, J. Enhanced Piezoresponse of Electrospun PVDF Mats with a Touch of Nickel Chloride Hexahydrate Salt. *Nanoscale* **2012**, *4*, 752−756.
(54) Yu, H.; Huang, T.; Lu, M.; Mao, M.; Zhang, Q.; Wang, H. Enhanced Power Output of an Electrospun PVDF/MWCNTs-Based Nanogenerator by Tuning its Conductivity. *Nanotechnology* **2013**, *24*, No. 405401.
(55) Baji, A.; Mai, Y.-W.; Li, Q.; Liu, Y. Electrospinning Induced Ferroelectricity in Poly (Vinylidene Fluoride) Fibers. *Nanoscale* **2011**, *3*, 3068−3071.
(56) Yee, W. A.; Kotaki, M.; Liu, Y.; Lu, X. Morphology, Polymorphism Behavior and Molecular Orientation of Electrospun Poly (Vinylidene Fluoride) Fibers. *Polymer* **2007**, *48*, 512−521.
(57) Mandal, D.; Yoon, S.; Kim, K. J. Origin of Piezoelectricity in an Electrospun Poly (Vinylidene Fluoride-Trifluoroethylene) Nanofiber Web-Based Nanogenerator and Nano-Pressure Sensor. *Macromol. Rapid Commun.* **2011**, *32*, 831−837.
(58) Lee, J. H.; Lee, K. Y.; Gupta, M. K.; Kim, T. Y.; Lee, D. Y.; Oh, J.; Ryu, C.; Yoo, W. J.; Kang, C. Y.; Yoon, S. J.; et al. Highly Stretchable Piezoelectric-Pyroelectric Hybrid Nanogenerator. *Adv. Mater.* **2014**, *26*, 765−769.
(59) Yang, Y.; Jung, J. H.; Yun, B. K.; Zhang, F.; Pradel, K. C.; Guo, W.; Wang, Z. L. Flexible Pyroelectric Nanogenerators Using a Composite Structure of Lead-Free $KNbO_3$ Nanowires. *Adv. Mater.* **2012**, *24*, 5357−5362.
(60) Wan, C.; Bowen, C. R. Multiscale-Structuring of Polyvinylidene Fluoride for Energy Harvesting: the Impact of Molecular-, Micro-and Macro-Structure. *J. Mater. Chem. A* **2017**, *5*, 3091−3128.
(61) Guo, W.; Tan, C.; Shi, K.; Li, J.; Wang, X.-X.; Sun, B.; Huang, X.; Long, Y.-Z.; Jiang, P. Wireless Piezoelectric Devices Based on Electrospun PVDF/$BaTiO_3$ NW Nanocomposite Fibers for Human Motion Monitoring. *Nanoscale* **2018**, *10*, 17751−17760.

https://dx.doi.org/10.1021/acsami.9b21392
ACS Appl. Mater. Interfaces 2020, 12, 8288−8295